

## Interference-Free Determination of the Optical Absorption Coefficient and the Optical Gap of Amorphous Silicon Thin Films

Yoshihiro HISHIKAWA, Noboru NAKAMURA, Shinya TSUDA,  
Shoichi NAKANO, Yasuo KISHI and Yukinori KUWANO

Functional Materials Research Center, SANYO Electric Co., Ltd., 1-18-13 Hashiridani, Hirakata, Osaka 573

(Received March 6, 1991; accepted for publication March 16, 1991)

A new method to determine the optical absorption coefficient ( $\alpha$ ) of thin films is presented.  $\alpha$  of hydrogenated amorphous silicon (a-Si:H) based alloys can be accurately determined from transmittance ( $T$ ) and reflectance ( $R$ ) by using  $T/(1-R)$ , which almost completely eliminates disturbance from the optical interference effect. The method is applicable to any thin films, as long as the film is a single layer. Based on the interference-free  $\alpha$ , various methods to determine the optical gap ( $E_{\text{OPT}}$ ) of a-Si:H, a-SiC:H, and a-SiGe:H films are discussed. The  $(n\alpha hv)^{1/3}$  plot and the  $(\alpha hv)^{1/3}$  plot are most suitable for characterizing these films. The well-known  $(\alpha hv)^{1/2}$  plot is less suited for detailed discussion of the  $E_{\text{OPT}}$  than the cube root plot, because the plot includes a large ambiguity in the  $E_{\text{OPT}}$ . The effect of the optical interference effect on the determination of the  $E_{\text{OPT}}$  is also discussed.

**KEYWORDS:** amorphous silicon, thin film, absorption coefficient, optical gap, bandgap, optical interference, SiC, SiGe

### §1. Introduction

The optical absorption coefficient ( $\alpha$ ) of hydrogenated amorphous silicon (a-Si:H) films is important for practical reasons, because it primarily determines the spectral response of opto-electric devices such as solar cells and photosensors. The  $\alpha$  also provides information on the electronic band structure, the band tail, and localized states.<sup>1)</sup> This practical and fundamental significance has led to a number of studies<sup>2)</sup> on the  $\alpha$  of a-Si:H and related alloys. However, experimental determination of  $\alpha$  is not a trivial task, mainly due to the existence of the optical interference effect. The  $\alpha$  of a-Si:H films in the visible and near IR region is usually determined from the optical transmittance ( $T$ ) and reflectance ( $R$ ).  $T$  and  $R$  can be expressed as functions of  $\alpha$  and the real part of the refractive index ( $n$ ).<sup>3)</sup> Conventional procedures to determine  $\alpha$  and  $n$  from the rigorous expressions of  $T$  and  $R$  are two-dimensional iterations in principle. Tomlin rearranged the expressions into simpler formulae.<sup>4)</sup> But solutions of  $\alpha$  and  $n$  were still complicated due to the existence of multiple solutions, especially at the maxima and minima of interference curves.<sup>5)</sup> Approaches to select the correct pair of  $\alpha$  and  $n$  required far more computation than to obtain the solutions.<sup>6)</sup> A few approximate formulae which are useful to determine  $\alpha$  more easily from  $T$  and  $R$  or  $T$  only have also been proposed.<sup>7-9)</sup> However, these approximate procedures usually restrict the spectral range or the sample thickness.

The  $\alpha$  also includes information on the separation between the valence band and the conduction band (optical gap:  $E_{\text{OPT}}$ ). In 1966, Tauc, Grigorovici, and Vancu<sup>10)</sup> first reported that  $h\nu(\epsilon_2)^{1/2}$ , which is proportional to  $(n\alpha hv)^{1/2}$ , of amorphous germanium (a-Ge) is represented by a straight line when plotted against the photon energy  $h\nu$ . Here,  $\epsilon_2$  denotes the imaginary part of the dielectric constant. Since then,  $E_{\text{OPT}}$  of tetrahedrally bonded amorphous semiconductors has usually been deduced by a linear extrapolation of the  $(\alpha hv)^{1/2}$  versus  $h\nu$  plot to the

energy axis. However, several experimental studies have revealed that there are other ways to determine the  $E_{\text{OPT}}$  with less experimental ambiguity. Cody, Brooks, and Abeles<sup>11)</sup> showed that the  $(\alpha/h\nu)^{1/2}$  versus  $h\nu$  plot of a-Si:H has better linearity than the  $(\alpha hv)^{1/2}$  plot, and thus includes less ambiguity of the  $E_{\text{OPT}}$ , in terms of the variation of sample thickness, than the  $(\alpha hv)^{1/2}$  plot. Vorlíček *et al.*,<sup>12)</sup> Klazes *et al.*,<sup>13)</sup> and Nitta *et al.*<sup>14)</sup> have reported that the  $(\alpha hv)^{1/3}$  or  $(n\alpha hv)^{1/3}$  versus  $h\nu$  plots of a-Si,<sup>12,13)</sup> a-Ge,<sup>12)</sup> and a-Si:H<sup>13,14)</sup> have better linearity than the  $(\alpha hv)^{1/2}$  plot. On the other hand, Kruzelecky *et al.* have recently reported that the  $(\alpha hv)^{1/2}$  plot of a-Si:H and a-Si films has two linear regions with different slopes.<sup>15)</sup> In other words, experimental data on the detailed energy dependence of  $\alpha$  are not in agreement at the present stage. Furthermore, the effect of the experimental error in  $\alpha$  on the  $E_{\text{OPT}}$  is not well known. From the practical point of view, it is desirable to identify which method provides the most reliable measurements to compare the optical properties of a-Si:H and related alloys with various compositions and thicknesses. The  $E_{\text{OPT}}$  is especially important in characterizing alloys such as hydrogenated amorphous silicon germanium (a-Si<sub>1-x</sub>Ge<sub>x</sub>:H), and hydrogenated amorphous silicon carbon (a-Si<sub>1-x</sub>C<sub>x</sub>:H), because their electrical and structural properties are strongly dependent on the  $E_{\text{OPT}}$ .

In this study, a new method to accurately determine the  $\alpha$  of thin films is presented. The new method is based on the finding which shows that the optical interference effect can be almost completely suppressed by using  $T/(1-R)$ . The  $E_{\text{OPT}}$  of a-Si:H films, a-Si<sub>1-x</sub>Ge<sub>x</sub>:H films, and a-Si<sub>1-x</sub>C<sub>x</sub>:H films are then investigated by the  $(\alpha hv)^{1/2}$  plot, the  $(\alpha hv)^{1/3}$  plot, the  $(n\alpha hv)^{1/3}$  plot, and the  $(\alpha/h\nu)^{1/2}$  plot. Attention is paid to the linearity of those plots and the experimental ambiguity of the deduced  $E_{\text{OPT}}$ .

### §2. Experimental Procedure

a-Si:H, a-Si<sub>1-x</sub>Ge<sub>x</sub>:H, and a-Si<sub>1-x</sub>C<sub>x</sub>:H films were

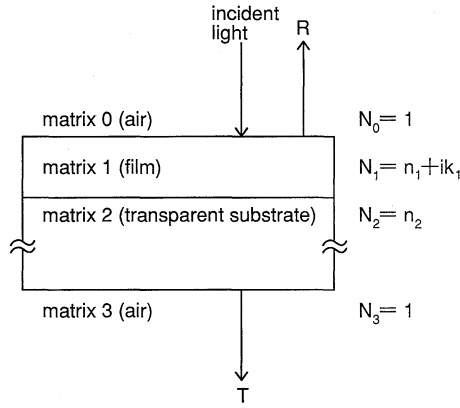


Fig. 1. Schematic structure of the samples used in this study.  $N_k$  denotes the complex refractive index of matrix  $k$ .

deposited on quartz or Corning #7059 glass substrates by RF Plasma Chemical Vapor Deposition (CVD) reactors.  $T$  and  $R$  were measured by a Hitachi U3400 spectrophotometer. Spectral resolution was 2 nm at 350~850 nm, and about 10 nm at 850~2000 nm. Light was incident on the film side (Fig. 1). An integrating sphere was used in order to avoid error in  $T$  and  $R$  due to diffuse light scattering of the samples. The  $T$  and  $R$  were measured at exactly the same position on each sample, which eliminates error in  $T$  and  $R$  caused by the variation of the film thickness. Aluminum mirrors, which were used to calibrate the 100%  $T$  and  $R$ , were also inserted in the optical path during the measurement of  $T$  and  $R$ , in order to cancel the spectral reflectance of the mirrors. Experimental error in  $T$  and  $R$  is better than  $\pm 1\%$  at 350~850 nm, and  $\pm 2\%$  at 850~2000 nm.

### §3. Suppression of Interference by $T/(1-R)$

Experimental data of  $T$ ,  $R$ , and  $T/(1-R)$  of (a) an a-Si:H film ( $d=1050$  nm) and (b) an a-Si<sub>1-x</sub>C<sub>x</sub>:H film ( $d=95$  nm) are shown in Fig. 2. Here,  $d$  denotes the thickness of the films. The interference effect is significant in  $T$  and  $R$  of both (a) and (b), which makes the determination of  $\alpha$  difficult. On the contrary,  $T/(1-R)$  is free from interference throughout the wavelength region in the figure, which is a new finding in this study. It is significant that this simple calculation almost completely eliminates the interference effect. This result suggests that  $T/(1-R)$  is very effective for determining  $\alpha$  in wavelength regions where the interference effect exists. That is,  $\alpha$  can be derived from a numerical fitting between experimental  $T/(1-R)$  and theoretical  $T/(1-R)$ .

Rigorous expressions of  $T$ ,  $R$ , and  $T/(1-R)$  for the structure in Fig. 1 are:

$$T = \frac{T_{23}T_{02}}{1 - R_{20}R_{23}}, \quad (1)$$

$$R = \frac{T_{20}^2 R_{23}}{1 - R_{20}R_{23}} + R_{02}, \quad (2)$$

$$\begin{aligned} \left(\frac{T}{1-R}\right)^{-1} &= \frac{(1-R_{02})(1-R_{20}R_{23}) - T_{20}^2 R_{23}}{T_{23}T_{02}} \\ &= \frac{1-R_{02}}{T_{23}T_{02}} - \frac{R_{23}}{T_{23}} \left( R_{20} \frac{1-R_{02}}{T_{02}} + T_{20} \right). \end{aligned} \quad (3)$$

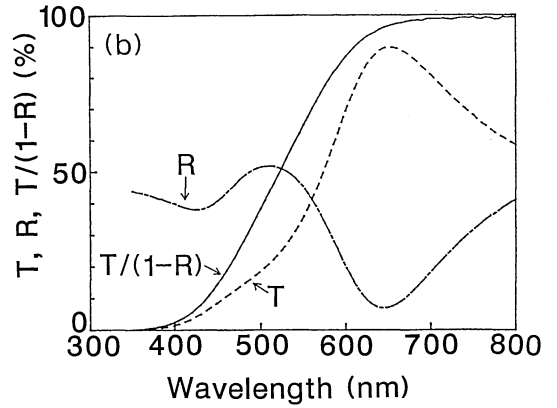
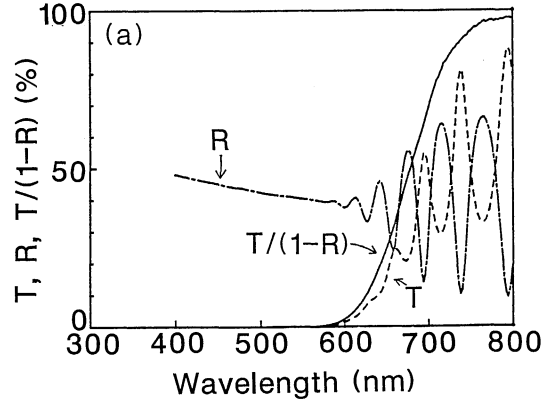


Fig. 2. Experimental transmittance ( $T$ ), reflectance ( $R$ ) and  $T/(1-R)$  of (a) an a-Si:H film with thickness = 1050 nm and (b) an a-Si<sub>1-x</sub>C<sub>x</sub>:H film with thickness = 95 nm.

Here,

$$T_{02} = T_{20} = \frac{n_2}{n_0} \left| \frac{e_1 t_{01} t_{12}}{1 - e_1^2 r_{10} r_{12}} \right|^2,$$

$$R_{02} = \left| r_{01} + \frac{e_1^2 t_{01} t_{10} r_{12}}{1 - e_1^2 r_{10} r_{12}} \right|^2,$$

$$R_{20} = \left| r_{21} + \frac{e_1^2 t_{21} t_{12} r_{10}}{1 - e_1^2 r_{12} r_{10}} \right|^2,$$

$$T_{23} = |t_{23}|^2 \frac{n_3}{n_2}, \quad R_{23} = |r_{23}|^2,$$

$$e_1 = \exp\left(\frac{2i\pi N_1 d}{\lambda}\right), \quad (4)$$

$$t_{kl} = \frac{2N_k}{N_k + N_l}, \quad r_{kl} = \frac{N_k - N_l}{N_k + N_l},$$

$N_k = n_k + ik_k$ : complex refractive index of matrix  $k$ .

Equation (3), in which all multiple reflections in the film as well as in the substrate are taken into account, is used for the determination of  $\alpha$  in this study. If the reflection at the substrate/air interface is neglected in eqs. (1)–(3), they are equivalent to similar expressions in ref. 4, when the substrate is transparent. The effect of suppressing interference using  $T/(1-R)$  can be understood as follows. For a typical value of  $n_2 = 1.5$ , the second term of eq. (3) is less than 4% of the first term, because  $R_{23} = 0.04$  and  $R_{20} + T_{20} < 1$ . Therefore eq. (3) can be written as:

$$\left(\frac{T}{1-R}\right)^{-1} \doteq \frac{1-R_{02}}{T_{23}T_{02}} = \frac{n_0(1-|r_{01}|^2)(e^{\alpha d} - e^{-\alpha d}|r_{12}|^2)}{n_3|t_{01}|^2|t_{12}|^2|t_{23}|^2} + \frac{4n_0|r_{01}||r_{12}|\sin(\theta+\gamma_{12})\sin(\gamma_{10})}{n_3|t_{01}|^2|t_{12}|^2|t_{23}|^2}. \quad (5)$$

Here,

$$\begin{aligned} \theta &= 4\pi n_1 d / \lambda, \\ \gamma_{12} &= \arg(r_{12}), \\ \gamma_{10} &= \arg(r_{10}), \\ d &: \text{film thickness,} \\ \lambda &: \text{wavelength.} \end{aligned}$$

The second term of eq. (5), which includes interference as  $\sin(\theta + \gamma_{12})$  is much smaller than the first term when  $k_1 \ll 1$ , because  $\sin \gamma_{10} \doteq 2k_1 / (n_1^2 - 1)$ . Here,  $k_1 = \lambda \alpha / 4\pi$ . Thus it has been confirmed that the interference effect in  $T/(1-R)$  is very small when  $k_1 \ll 1$ . Even when  $k_1 \sim 1$ ,  $T/(1-R)$  is practically effective for the interference-free determination of  $\alpha$ , which will be demonstrated in later examples.

#### §4. Determination of the Optical Absorption Coefficient ( $\alpha$ )

When the  $n_1$  (real part of the refractive index of the film),  $d$  (thickness of the film), and the experimental value of  $T/(1-R)$  are known,  $\alpha$  can be easily determined from eq. (3) by simple iterative calculation such as Newton's method. When  $n_1$  and  $d$  are not known, they can be determined together with  $\alpha$  from  $T/(1-R)$  and  $R$  by the following procedure (Fig. 3). First, rough values of  $n_1$  and  $d$  are estimated. Then  $\alpha$  is iteratively deter-

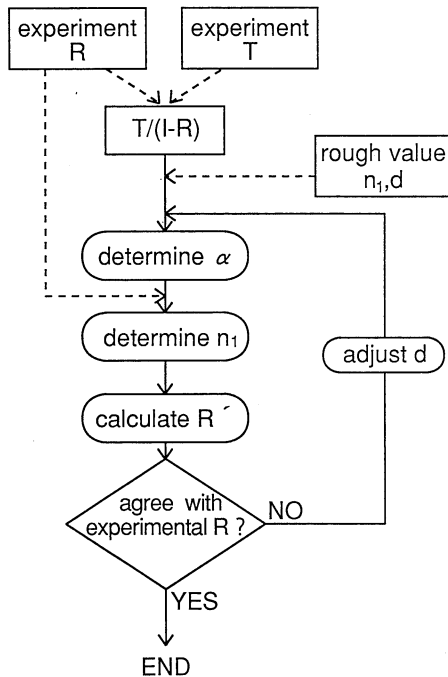


Fig. 3. Procedure used to determine the optical absorption coefficient ( $\alpha$ ) from experimental transmittance ( $T$ ) and reflectance ( $R$ ).

mined by using eq. (3) from  $T/(1-R)$ ,  $n_1$ , and  $d$ . Next, the values of  $n_1$  at the wavelengths where  $R$  has interference maxima, are also iteratively determined by using eq. (2) from  $R$ ,  $\alpha$ , and  $d$ . At those interference maxima, eq. (4) can be rewritten as  $e_1 = \exp(2i\pi N_1 d / \lambda) = \pm i \cdot \exp(-\alpha/2)$ , which should be used in the calculation. Finally, eq. (2) is used to calculate reflectance ( $R'$ ) from determined  $\alpha$  and  $n_1$ . Here, the spectral response of  $n_1$  is approximated by a linear interpolation based on the values of  $n_1$ , which are determined at the wavelengths of reflectance maxima.  $R'$  and experimental  $R$  are then compared in order to check whether  $\alpha$ ,  $n_1$ , and  $d$  are properly determined. If  $R'$  and  $R$  do not agree well, the value of  $d$  is adjusted, and the same procedure is carried out until good agreement is obtained. Figure 4 shows  $\alpha$  of the same samples as Fig. 2, which is determined by the above procedure. It is clearly seen that  $\alpha$  can be determined practically free from the interference effect. When  $R$  has several interference maxima,  $\alpha$ ,  $n_1$  (at the wavelength of reflectance maxima), and  $d$  can be accurately determined by the above procedure. As a result, experimental  $R$  and  $T$  are very well reproduced by using eqs. (1) and (2) from determined  $\alpha$ ,  $n_1$ , and  $d$  (Fig. 5). In this case, the total accuracy of  $\alpha$  is limited by the experimental error in  $T$  and  $R$ . When  $R$  has only a few maxima or less, the data of  $n_1$ , determined at the reflectance maxima, are not enough to estimate the whole spectral response of  $n_1$ . However, even if  $n_1$  is misestimated, the error in the determined  $\alpha$  is not large. A typical example is also shown in Fig. 4, in which misestimation of  $n_1$  by 0.5 results in the error in  $\alpha$  of about 10%.

Figure 6(a) shows  $\alpha$  of a-Si:H films with different  $d$ . Deposition conditions of the films are the same, and  $d$  is controlled by changing the deposition time. The  $\alpha$  is almost the same for all films, and is slightly smaller in thinner films.<sup>16)</sup>  $\alpha$  can be accurately determined regardless of  $d$  throughout the wavelength region in Fig. 6(a). It should be noted that if the interference effect is not suppressed, the error in  $\alpha$  is very large. For example,

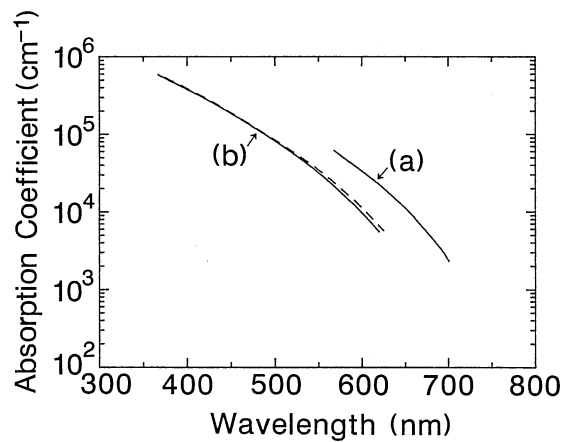


Fig. 4. Optical absorption coefficient ( $\alpha$ ) determined from the experimental  $T$  and  $R$  in Fig. 2, by using the procedure in Fig. 3. Lines denoted as (a) and (b) in the figure correspond to the experimental data in Figs. 2(a) and 2(b), respectively. The broken line shows  $\alpha$  when the refractive index  $n_1$  is underestimated by 0.5, as compared to the solid line.

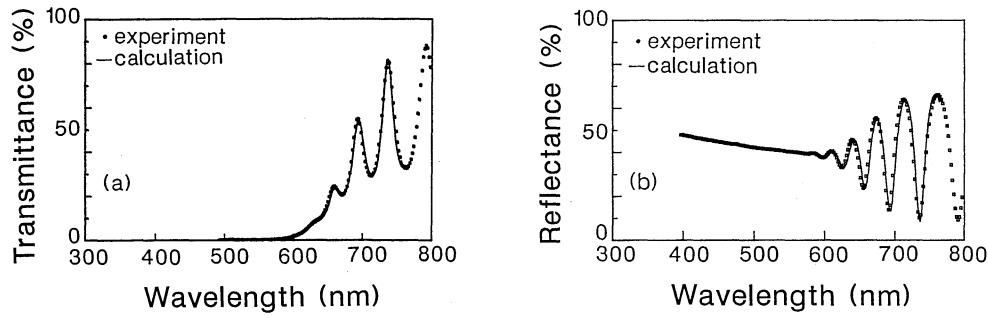


Fig. 5. Comparison of experiment and calculation of (a) transmittance ( $T$ ) and (b) reflectance ( $R$ ). The sample is the same as in Fig. 2(a). Experimental  $T$  and  $R$  are denoted by dots. Calculated  $T$  and  $R$  from the determined  $\alpha$ ,  $n_1$ , and  $d$  are denoted by lines.

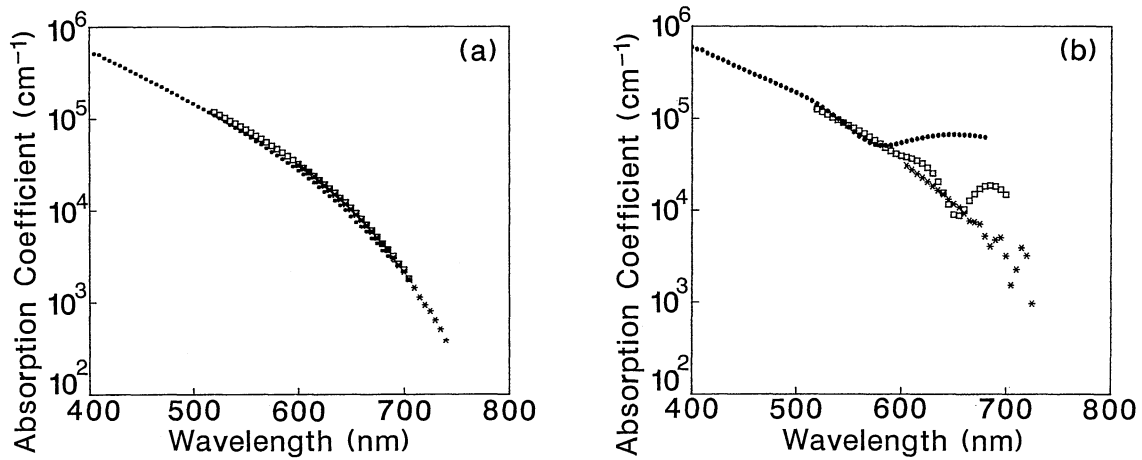


Fig. 6. The  $\alpha$  of a-Si:H films with different thicknesses; ( $\bullet$ )  $d=130$  nm, ( $\square$ )  $d=260$  nm, ( $*$ )  $d=2250$  nm. The  $\alpha$  is determined (a) accurately by the procedure in this study, and (b) from  $T$  only. Deposition conditions are identical for the three films. Film thickness is controlled by the deposition time.

Fig. 6(b) shows  $\alpha$ , determined from  $T$  only based on the same experimental data as in Fig. 6(a), by using the following formula:

$$T = (1 - r) \exp(-\alpha d).$$

Here,

$$r = (n_1 - 1) / (n_1 + 1). \quad (6)$$

The  $\alpha$  in Fig. 6(b) apparently has a large error due to the interference effect. Averaging the interference fringes does not result in an accurate  $\alpha$ . The error in  $\alpha$  leads to even more serious problems in the determination of  $E_{\text{OPT}}$ , as will be discussed later.

### §5. Optical Gap ( $E_{\text{OPT}}$ )

The  $\alpha$  of a-Si:H, a-Si $_{1-x}$ C $_x$ :H, and a-Si $_{1-x}$ Ge $_x$ :H films with different compositions are shown in Fig. 7. Symbols are listed in Table I. Figure 8(a) shows  $(n\alpha hv)^{1/3}$  as functions of  $hv$ . The linearity of the plots is good for all the samples. This agrees with previous reports on a-Si,<sup>12,13</sup> a-Ge,<sup>12</sup> and a-Si:H.<sup>13,14</sup> Although there is small change in the slope, the plots are well approximated by linear lines where  $(n\alpha hv)^{1/3} < 100$  ( $\text{cm}^{-1} \cdot \text{eV}$ )<sup>1/3</sup>. This result suggests that the good linearity of the  $(n\alpha hv)^{1/3}$  versus  $hv$  plot is a common feature of a-Si:H, a-Si $_{1-x}$ C $_x$ :H, and

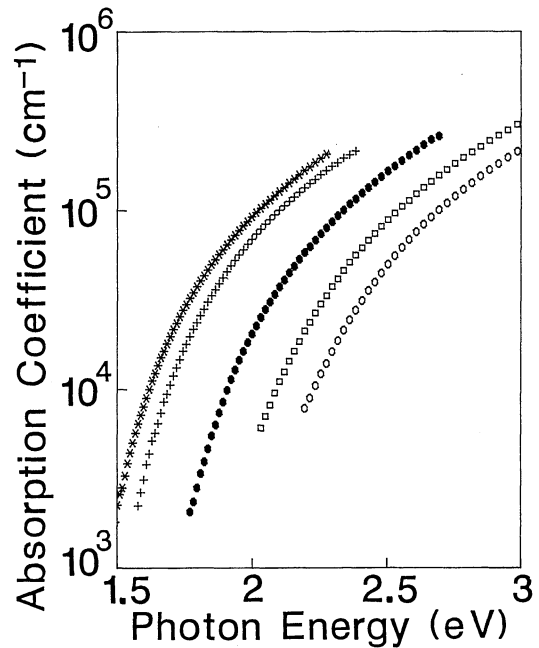


Fig. 7. The  $\alpha$  of an a-Si:H film ( $\bullet$ ), a-Si $_{1-x}$ C $_x$ :H films ( $\square$ ,  $\circ$ ), and a-Si $_{1-x}$ Ge $_x$ :H films ( $*$ ,  $+$ ). Deposition conditions and optical properties of the films are listed in Table I.

Table I. Deposition conditions and optical properties of a-Si:H, a-SiC:H, and a-SiGe:H. The range of  $E_{OPT3}$ ,  $E_{OPT2}$ ,  $B_3$ , and  $B_2$  indicates the differences in those values when linear extrapolation is carried out at around  $(n\alpha h\nu)^{1/3}=100$  and at around the low energy edge of the experimental data in Fig. 8.

Sample No.	Symbol	Material	Source gas	RF power (mW/cm <sup>2</sup> )	Thickness (nm)	$E_{OPT3}^{a)}$ (eV)	$E_{OPT2}^{b)}$ (eV)	$B_3^{c)}$ (cm <sup>-1</sup> eV <sup>-2</sup> ) <sup>1/3</sup>	$B_2^{d)}$ (cm <sup>-1</sup> eV <sup>-1</sup> ) <sup>1/2</sup>
1	●	a-Si:H	100% SiH <sub>4</sub>	25	260	1.59~1.60	1.69~1.80	86~88	650~900
2	□	a-SiC:H	[CH <sub>4</sub> ]/[SiH <sub>4</sub> ]=2	30	100	1.75	1.88~1.97	78~79	680~870
3	○	a-SiC:H	[CH <sub>4</sub> ]/[SiH <sub>4</sub> ]=4	30	80	1.87~1.88	2.01~2.10	75~77	680~860
4	*	a-SiGe:H	[GeH <sub>4</sub> ]/[SiH <sub>4</sub> ]=0.15	25	300	1.31~1.34	1.41~1.50	86~92	610~860
5	+	a-SiGe:H	[GeH <sub>4</sub> ]/[SiH <sub>4</sub> ]=0.03	25	270	1.38~1.41	1.50~1.57	86~94	670~850

<sup>a)</sup>optical gap determined from an  $(n\alpha h\nu)^{1/3}$  versus  $h\nu$  plot

<sup>b)</sup>optical gap determined from an  $(\alpha h\nu)^{1/2}$  versus  $h\nu$  plot

<sup>c)</sup>slope of an  $(n\alpha h\nu)^{1/3}$  versus  $h\nu$  plot

<sup>d)</sup>slope of an  $(\alpha h\nu)^{1/2}$  versus  $h\nu$  plot

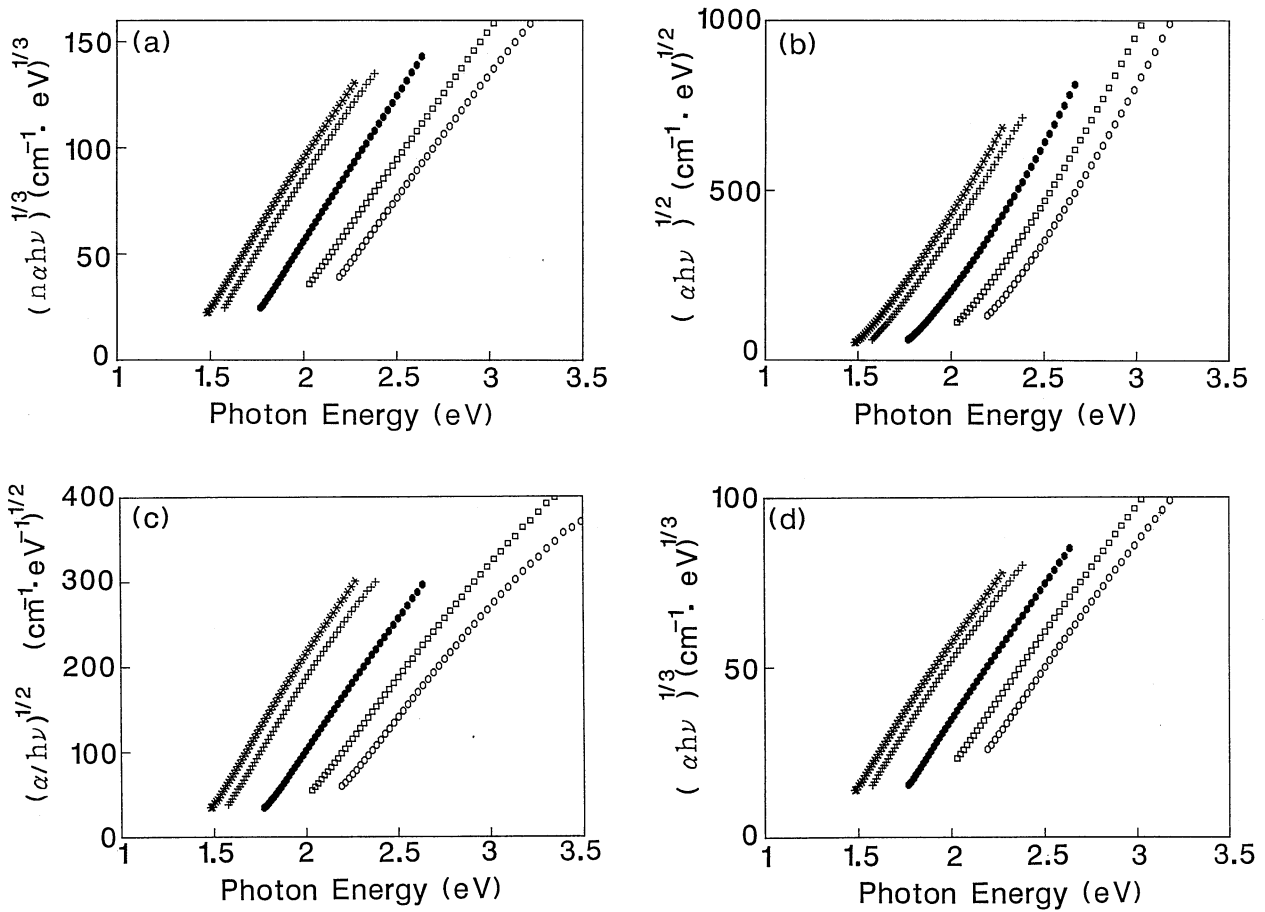


Fig. 8. The (a)  $(n\alpha h\nu)^{1/3}$  plot, (b)  $(\alpha h\nu)^{1/2}$  plot, (c)  $(\alpha/h\nu)^{1/2}$  plot, and (d)  $(\alpha h\nu)^{1/3}$  plot of an a-Si:H film (●), a-Si<sub>1-x</sub>C<sub>x</sub>:H films (□, ○), and a-Si<sub>1-x</sub>Ge<sub>x</sub>:H films (\*, +). Samples are the same as in Fig. 7.

a-Si<sub>1-x</sub>Ge<sub>x</sub>:H alloys. In other words,  $\alpha$  near the optical absorption edge can be well approximated by

$$\alpha = (B_3(h\nu - E_{OPT3}))^3 / nh\nu. \quad (7)$$

Here,  $E_{OPT3}$  is the optical gap and  $B_3$  is a constant. These values are also listed in Table I. The spectral range where  $(n\alpha h\nu)^{1/3} < 100$  (cm<sup>-1</sup>·eV)<sup>1/3</sup> corresponds to  $\alpha$  on the order of  $10^3 \sim 10^4$  cm<sup>-1</sup>. This is technologically important, because the spectral response of solar cells and photodetectors are sensitive to  $\alpha$  in that range. The  $(\alpha h\nu)^{1/2}$  versus  $h\nu$  plots of the same samples, on the con-

trary, do not have linear regions, as shown in Fig. 8(b). Therefore, ambiguity is inevitable if the  $E_{OPT}$  is determined by the  $(\alpha h\nu)^{1/2}$  plot, which is also listed in Table I. The  $(\alpha/h\nu)^{1/2}$  versus  $h\nu$  plots (Fig. 8(c)) show better linearity than the  $(\alpha h\nu)^{1/2}$  plots. This result is in agreement with Cody, Brooks, and Abeles.<sup>11)</sup> However, linearity of the  $(n\alpha h\nu)^{1/3}$  plot is best among the three kinds of plots (Figs. 8(a)~8(c)) in this study, which means that the experimental ambiguity in determining the  $E_{OPT}$  is smallest in the  $(n\alpha h\nu)^{1/3}$  plot. The  $(\alpha h\nu)^{1/3}$  versus  $h\nu$  plot has almost the same linearity (Fig. 8(d)). It results in

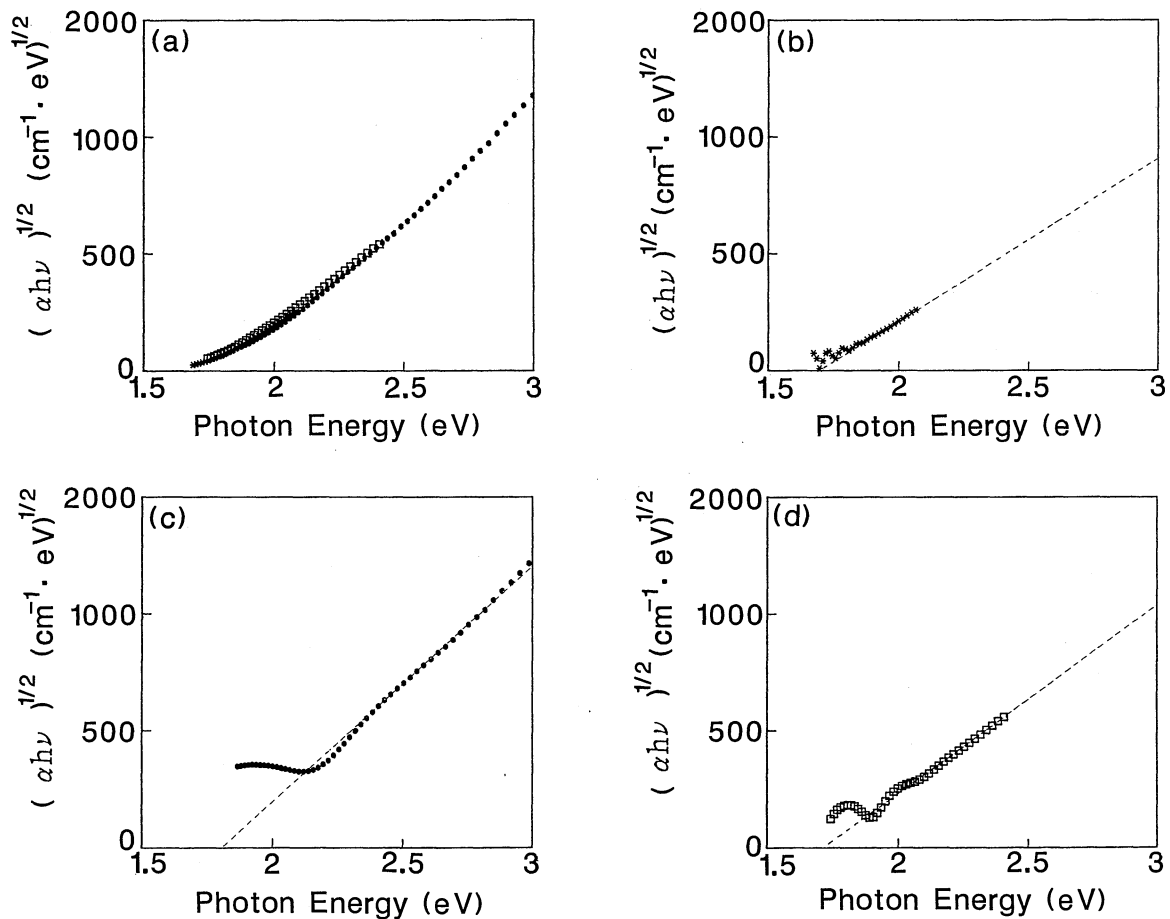


Fig. 9. The  $(\alpha h\nu)^{1/2}$  plots of a-Si:H films. Samples are the same as in Fig. 6. The  $\alpha$  is determined (a) accurately by the procedure in this study, and (b)–(d) from  $T$  only. The plots in (b)–(d) appear as if they have linear regions, as indicated by dashed lines. However, they are the artifacts of the errors in  $\alpha$  caused by the optical interference effect, and do not have physical significance.

slightly smaller (by about 10 meV)  $E_{\text{OPT}}$  as compared to the  $(n\alpha h\nu)^{1/3}$  plot, when the spectral range of  $(n\alpha h\nu)^{1/3} < 100 \text{ (cm}^{-1} \cdot \text{eV)}^{1/3}$  is used. This is in qualitative agreement with the results of Klazes *et al.*<sup>13)</sup>

Care should be taken in the accuracy of  $\alpha$ , because the error in  $\alpha$  significantly alters the shape of the plots. Especially, the error in  $\alpha$  which is due to the interference effect usually makes the  $(\alpha h\nu)^{1/2}$  plots appear as if they have linear regions. This leads to a serious misestimation of the optical gap. Figure 9 shows the  $(\alpha h\nu)^{1/2}$  plots of the same samples as Fig. 6. The plots do not have linear regions when an accurate  $\alpha$  is used (Fig. 9(a)). The plots seem to have linear regions when the error in  $\alpha$  exists (Figs. 9(b)–9(d)). Of course, the appearance of linear regions in Figs. 9(b)–9(d) is the artifact of the error in  $\alpha$ , and does not have physical significance.

## §6. Discussion

The procedure used to determine  $\alpha$  in this study has the primary advantage that  $\alpha$  can be determined without disturbance from the interference effect by using  $T/(1-R)$ . Furthermore, the calculation included in the procedure is a simple one-dimensional iteration, which requires much less calculation time than the two-dimensional iteration in conventional procedures<sup>4-6)</sup> to deter-

mine  $\alpha$  from  $T$  and  $R$ . The spectral response of refractive index  $n_1$  should be estimated based on experimental  $R$ , in order to determine  $\alpha$ . However, the error in the determined  $\alpha$  is typically about 10%, even when the misestimation of  $n_1$  is 0.5, as mentioned above. If one tries to determine both  $\alpha$  and  $n_1$  at all the wavelengths at which  $T$  and  $R$  are measured, the problem of double solutions and missing solutions is inevitable, because the solutions of  $\alpha$  and  $n_1$  are very sensitive to small experimental errors in  $T$  and  $R$  at the minima and maxima of interference curves.<sup>6)</sup> This leads to the error in the determined  $\alpha$ . Especially when there is experimental error in  $T$  and  $R$  due to the diffuse light scattering of the samples, variations in film thickness, or limited spectral resolution of the measurement apparatus, the error in  $T$  and  $R$  is large at the minima and maxima of  $T$  and  $R$ , because the interference curves are partly smeared. This can lead to serious error in  $\alpha$ . On the other hand, such experimental error in  $T$  and  $R$  barely affects  $T/(1-R)$ , because the errors in  $T$  and  $R$  are cancelled. Therefore, the procedure to determine  $\alpha$  in this study has an advantage over conventional methods when such experimental error exists. The above feature of  $T/(1-R)$  is important for the optical characterization of amorphous silicon based alloys, because films with various compositions and thicknesses

can be treated without influence from the interference effect. In this study, this feature is utilized for a detailed comparison of the various methods which were proposed to determine the  $E_{\text{OPT}}$ .

Based on interference-free  $\alpha$ , the  $(n\alpha hv)^{1/3}$  versus  $hv$  plot can determine the  $E_{\text{OPT}}$  with much less ambiguity than the  $(\alpha hv)^{1/2}$  plot for all the a-Si:H, a-Si<sub>1-x</sub>Ge<sub>x</sub>:H, and a-Si<sub>1-x</sub>C<sub>x</sub>:H films in this study. If the  $E_{\text{OPT}}$  of these films is determined by the  $(\alpha hv)^{1/2}$  plot, ambiguity is inevitable. A previous study<sup>11)</sup> showed that the  $(\epsilon_2 E^2)^{1/2}$ , which is proportional to  $(n\alpha hv)^{1/2}$ , includes ambiguity of the  $E_{\text{OPT}}$  by  $\sim 300$  meV when the film thickness and the extrapolated energy range are not specified. The present study has clarified that the ambiguity of  $\sim 100$  meV exists even when the linearly extrapolated energy region and the film thickness are specified as in Table I. On the contrary, one can determine the  $E_{\text{OPT}}$  within an error of 10 meV by the  $(n\alpha hv)^{1/3}$  plot or the  $(\alpha hv)^{1/3}$  plot, when the energy range where  $(n\alpha hv)^{1/3} < 100$  (cm<sup>-1</sup>·eV)<sup>1/3</sup> is used. These results are in qualitative agreement with several previous studies,<sup>11-14)</sup> in which  $\alpha$  is carefully determined. Considering this, it is rather surprising that the  $(\alpha hv)^{1/2}$  plot has been widely used to determine the  $E_{\text{OPT}}$  of amorphous silicon-based alloys. The present study has also revealed that the error in  $\alpha$ , due to the optical interference effect, makes the  $(\alpha hv)^{1/2}$  plot appear to have linear regions. This is probably one of the reasons why the plot is used to determine the  $E_{\text{OPT}}$ . Demichelis *et al.*<sup>8)</sup> also discussed various methods to determine the  $E_{\text{OPT}}$ . However, the difference in the linearity of the plots was not reported, probably because the data on  $\alpha$  included errors due to the optical interference effect. The interference effect is not satisfactorily suppressed in the experimental  $\alpha$  of ref. 8. There have been discussions on the relations between the  $E_{\text{OPT}}$  and the density of states of the electronic bands,<sup>17)</sup> the mobility gap,<sup>18)</sup> the optical transition matrix element,<sup>11)</sup> and photoluminescence spectra.<sup>14)</sup> These studies are of course important in understanding the electronic structure of the materials. However, the necessity of minimizing the experimental ambiguity of the  $E_{\text{OPT}}$  is another important consideration. For example, the photoconductivity ( $\sigma_{\text{PH}}$ ) of amorphous silicon based alloys sometimes varies by a few orders when the  $E_{\text{OPT}}$  varies by 100 meV. Therefore, the experimental ambiguity of the  $E_{\text{OPT}}$  should be well below 100 meV, in order to obtain valid results and discuss the  $\sigma_{\text{PH}}$  in detail. Small ambiguity in the  $E_{\text{OPT}}$ , as determined by the cube root plots, will be necessary for further study on the optical and electronic properties of amorphous silicon based alloys.

## §7. Conclusions

The optical absorption coefficient ( $\alpha$ ) of a-Si:H, a-Si<sub>1-x</sub>Ge<sub>x</sub>:H, and a-Si<sub>1-x</sub>C<sub>x</sub>:H films can be accurately determined by using  $T/(1-R)$ , without being disturbed by the optical interference effect. The calculation time re-

quired to determine  $\alpha$  is much shorter than that designated in conventional methods. The procedure used to determine  $\alpha$  in this study is applicable to any thin film regardless of the material and thickness, as long as the film is a single layer. Based on interference-free  $\alpha$ , it has been concluded that the  $(n\alpha hv)^{1/3}$  versus  $hv$  plot and the  $(\alpha hv)^{1/3}$  versus  $hv$  plot have the best linearity among the various methods to determine the optical gap ( $E_{\text{OPT}}$ ), for all the samples in this study. The difference in the  $E_{\text{OPT}}$  between the two plots is only  $\sim 10$  meV when the spectral range of  $(n\alpha hv)^{1/3} < 100$  (cm<sup>-1</sup>·eV)<sup>1/3</sup> is used for the linear fitting. On the contrary, the  $E_{\text{OPT}}$  determined by the  $(\alpha hv)^{1/2}$  plot includes ambiguity of  $\sim 100$  meV or more, unless the linearly extrapolated range is very strictly specified. Therefore, it is less suited for detailed characterization of amorphous silicon-based alloys than the cube root plots. Care should be taken with the accuracy of  $\alpha$  in determining the  $E_{\text{OPT}}$ , because the error in  $\alpha$  due to the optical interference effect makes the  $(\alpha hv)^{1/2}$  plots appear as if they have linear regions.

## Acknowledgements

The authors are grateful to S. Okamoto for stimulating discussion. This work is supported by NEDO as a part of the Sunshine Project under the Ministry of International Trade and Industry.

## References

- 1) J. I. Pankove: *Solar Cells* **24** (1988) 299.
- 2) *Semiconductors and Semimetals* ed. J. I. Pankove (Academic Press, Orland, 1984) Vol. 21B.
- 3) O. S. Heavens: *Optical Properties of Thin Solid Films* (Butterworth, London, 1955).
- 4) S. G. Tomlin: *J. Phys. D* **2** (1968) 1667.
- 5) R. E. Denton, R. D. Campbell and S. G. Tomlin: *J. Phys. D* **5** (1972) 852.
- 6) R. C. McPhedran, L. C. Botten, D. R. McKenzie and R. P. Netterfield: *Appl. Opt.* **23** (1984) 1197.
- 7) D. Ritter and K. Weiser: *Opt. Commun.* **57** (1986) 336.
- 8) F. Demichelis, E. Minetti-Mezzetti, A. Tagliaferro and E. Tresso: *J. Appl. Phys.* **59** (1986) 611.
- 9) R. Swanepoel: *J. Phys. E* **16** (1983) 214.
- 10) J. Tauc, R. Grigorovici and A. Vancu: *Phys. Status Solidi* **15** (1966) 627.
- 11) G. D. Cody, B. G. Brooks and B. Abels: *Sol. Energy Mater.* **8** (1982) 231.
- 12) V. Vorlíček, M. Závětová, S. K. Pavlov and L. Pajasová: *J. Non-Cryst. Solids* **45** (1981) 289.
- 13) R. H. Klazes, M. H. L. M. van der Broek, J. Bezemer and S. Radelaar: *Philos. Mag.* **45** (1982) 377.
- 14) S. Nitta, S. Itoh, M. Tanaka, T. Endo and A. Hatano: *Sol. Energy Mater.* **8** (1982) 249.
- 15) R. V. Kruzelecky, C. Ukah, D. Rakanski and S. Zukotynski: *J. Non-Cryst. Solids* **103** (1988) 234.
- 16) Y. Hishikawa, S. Tsuge, N. Nakamura, S. Tsuda, S. Nakano and Y. Kuwano: *Appl. Phys. Lett.* **57** (1990) 771.
- 17) W. B. Jackson, S.-J. Oh, C. C. Tsai and J. W. Allen: *Phys. Rev. Lett.* **53** (1984) 1481.
- 18) C. R. Wronski, S. Lee, M. Hicks and Satyendra Kumar: *Phys. Rev. Lett.* **63** (1989) 1420.